

# Similarity laws of the fiber-matrix interface crack in Fiber-Reinforced Polymer Composites

Luca Di Stasio<sup>a,b</sup>, Janis Varna<sup>a</sup>, Zoubir Ayadi<sup>b</sup>

<sup>a</sup>*Luleå University of Technology, University Campus, SE-97187 Luleå, Sweden*

<sup>b</sup>*Université de Lorraine, EEIGM, IJL, 6 Rue Bastien Lepage, F-54010 Nancy, France*

---

## Abstract

*Keywords:* Fiber Reinforced Polymer Composite (FRPC), Debonding,  
Similarity, Dimensional analysis

---

## 1. Introduction

One of the most promising developments in Fiber Reinforced Polymer Composites (FRPCs) for advanced structural applications is currently represented by *thin-ply* laminates [1]. Constituted by extremely thin plies, with  $t_{90^\circ}$  as  
5 small as just  $\sim 4 - 5$  fiber diameters, this family of laminates is characterized by its damage tolerance, in particular the capability of delaying to higher strains and even suppressing the onset and propagation of transverse cracks [2]. The recent experimental assessment of transverse cracks suppression in *thin-ply* laminates [3, 4, 5] validates the existence of a *ply-thickness* effect [5] at scales  
10  $10x$  smaller than those at which it was originally observed at the end of the 1970's [6].

Onset of transverse cracks coincides at the microscopic level with the formation of fiber/matrix interface cracks [7], or debonds. After the inter-fiber stress [8] and strain concentration [9] causes the matrix to fail at or close to the fiber in-  
15 terface, debonds grow along the fiber arc direction until a maximum or critical size is reached. If the applied load is increased, debonds move into the matrix or

“kink” out of the fiber/matrix interface [10, 11]. Coalescence of debonds then occurs, which corresponds macroscopically to through-the-thickness transverse crack propagation [10, 12]. Finally, propagation through the specimen width  
20 occurs [10].

Given that *thin-ply*s, as previously noted, can reach nowadays thicknesses of just  $\sim 4 - 5$  fiber diameters, the characteristic size of the ply, i.e. the thickness  $t_{90^\circ}$ , is now comparable in magnitude to the characteristic size of debonds, i.e. the fiber diameter  $2R_f$ , such that  $t_{90^\circ}/(2R_f) \sim \mathcal{O}(1)$ . This has motivated  
25 in recent years a renewed interest in debond growth modeling [13, 14, 15, 16]. Since the elastic solution to the interface crack problem implies an oscillating solution at the crack tip [17] in the *open* case (crack faces not in contact), Stress Intensify Factors (SIFs) are not defined and debond growth characterization has focused on the determination of Mode I, Mode II and total Energy Release Rate  
30 (ERR). Many authors have reported their results in normalized form [11, 18, 19], by defining a reference ERR  $G_0$ . The definition of such reference ERR would be useful to establish similarity laws and thus to allow comparisons between different material systems, scales, loads and microstructural arrangement. However, no agreement can be found in the literature on the very definition of  $G_0$  and  
35 expressions vary between authors. Furthermore, no clear derivation of  $G_0$  has been proposed. In this brief contribution, we provide a derivation of  $G_0$  based on arguments of dimensional analysis, material homogenization and fracture mechanics; we then apply the derived expression of reference ERR to the analysis of debond growth in Representative Volume Elements (RVEs) of UD composites  
40 and cross-ply laminates.

## 2. Dimensional analysis

We first recall that the Energy Release Rate  $G$  has units of energy  $E$  per unit area:

$$[G] = \frac{E}{L^2}, \quad (1)$$

where  $L$  stands for unit of length. By algebraic manipulation of Equation 1  
 45 we can write the units of ERR as

$$\frac{E}{L^2} = \frac{F \cdot L}{L^2} = \frac{F}{L^2} \frac{L}{L}, \quad (2)$$

where  $F$  stands for unit of force. We recognize that, in Equation 2

$$\frac{F}{L^2} = [\sigma] \quad \frac{L}{L} = [\varepsilon], \quad (3)$$

where  $\sigma$  and  $\varepsilon$  are respectively stress and strain. The reference Energy Release Rate is thus dimensionally equivalent to a reference stress  $\sigma_{ref}$  times a reference strain  $\varepsilon_{ref}$  times a reference length  $l_{ref}$  and we can write

$$G_0 \sim \sigma_{ref} \varepsilon_{ref} l_{ref}. \quad (4)$$

### 50 **3. Linear Elastic Fracture Mechanics (LEFM) considerations**

In the case of uniaxial loading, we can assume that: in a stress-controlled experiment,  $\sigma_{ref}$  is equal to the applied stress  $\sigma_0$  and  $\varepsilon_{ref}$  to the average strain  $\varepsilon_0$  in the Representative Volume Element (RVE); in a strain-controlled experiment,  $\varepsilon_{ref}$  is equal to the applied strain  $\varepsilon_0$  and  $\sigma_{ref}$  to the average stress  $\sigma_{av}$   
 55 in the Representative Volume Element (RVE).

Under the assumption of linear elastic material constituents, we have, respectively for a stress- and strain-controlled experiment:

$$\varepsilon_{av} = E_{homo} \sigma_0 \quad \sigma_{av} = E_{homo} \varepsilon_0, \quad (5)$$

where  $E_{homo}$  is a homogenized RVE Young's modulus which measures the RVE elastic response in the presence of different material phases and damage.  
 60 It is worth to point out here that, as we are interested in studying debond growth in the context of transverse crack onset, RVEs are loaded in the direction transverse to the fibers in the layer where debonds are present. Furthermore, we consider RVEs that are 2-dimensional and under the assumption of plane

strain or plane stress conditions. This implies, considering the elastic response  
65 of a transversely isotropic material in its plane of transverse isotropy (indeces  
2 – 3, index 1 corresponds to the axis of rotational symmetry) with no damage,  
that [20, 21]

$$E_{homo} = \frac{E_2}{1 - \nu_{12}\nu_{21}} \quad E_{homo} = E_2, \quad (6)$$

respectively for plane strain and plane stress, with  $E_2$  the homogenized trans-  
verse Young's modulus of the ply and  $\nu_{12}$ ,  $\nu_{21}$  the major and minor Poisson's  
70 ratios. Notice that homogenized elastic properties depend on constituents' elas-  
tic properties and theIn the presence of damage, we can assume the homoge-  
nized Young's modulus of the damaged RVE to be a fraction of the undamaged  
modulus  $E_{homo}^0$  (expressed in Eq. 6):

$$E_{homo} = f(\Delta\theta) E_{homo}^0, \quad (7)$$

where  $0 < f(\Delta\theta) < 1$  is a function of the damage state in the material,  
75 in this case represented by the debond half-size  $\Delta\theta$  (debond size is  $2\Delta\theta$ ). By  
substituting Eq. 5, Eq. 6 and Eq. 7 in Eq. 4, we have

$$G_0 \sim f(\Delta\theta) \frac{E_2}{1 - \nu_{12}\nu_{21}} \varepsilon_0^2 l_{ref} \quad G_0 \sim f(\Delta\theta) E_2 \varepsilon_0^2 l_{ref}, \quad (8)$$

respectively for plane strain and plane stress conditions under applied strain  
 $\varepsilon_0$ , and

$$G_0 \sim f(\Delta\theta) \frac{1 - \nu_{12}\nu_{21}}{E_2} \sigma_0^2 l_{ref} \quad G_0 \sim f(\Delta\theta) \frac{\sigma_0^2}{E_2} l_{ref}, \quad (9)$$

respectively for plane strain and plane stress conditions under applied strain  
80  $\sigma_0$ . Notice that, incidentally: the plane strain expression in Eq. 9 is the same  
as the ERR expression used for *in-situ* strenght modeling in [22] and derived  
in [23] by considering the fiber-reinforced polymer as a 3-phase composite with

one phase constituted by sharp voids (cracks)<sup>1</sup>; the plane stress expression in Eq. 9 is the same as the Mode I ERR in [24], derived from the definition of ERR  
85 and problem geometry.

In accord with the classic Linear Elastic Fracture Mechanics (LEFM), the Energy Release Rate is directly proportional to the crack size  $a$  [25]. Given that  $a = R_f 2\Delta\theta$  for debonds, where  $R_f$  is the fiber radius, it is reasonable to assume  $R_f$  as the reference length:

$$l_{ref} = R_f. \quad (10)$$

90 The reference Energy Release Rate thus becomes

$$G_0 \sim f(\Delta\theta) \frac{E_2}{1 - \nu_{12}\nu_{21}} \varepsilon_0^2 R_f \quad G_0 \sim f(\Delta\theta) E_2 \varepsilon_0^2 R_f, \quad (11)$$

respectively for plane strain and plane stress conditions under applied strain  $\varepsilon_0$ , and

$$G_0 \sim f(\Delta\theta) \frac{1 - \nu_{12}\nu_{21}}{E_2} \sigma_0^2 R_f \quad G_0 \sim f(\Delta\theta) \frac{\sigma_0^2}{E_2} R_f, \quad (12)$$

respectively for plane strain and plane stress conditions under applied strain  $\sigma_0$ .

#### 95 4. Similarity and geometry correction factor

In agreement with the classic Fracture Mechanics (FM) treatment [25], we can recognize in the function  $f(\Delta\theta)$  of Eq. 11 and Eq. 12 the geometry correction factor ( $f(a)$  or  $Y$ ) that establishes the relation of similarity [26]

$$K = f(a) \sigma \sqrt{a} \quad \text{or} \quad G = f^2(a) \frac{\sigma^2}{E} a \quad (13)$$

---

<sup>1</sup>Often expressed as  $\Lambda_{22}^0 = 2 \left( \frac{1}{E_2} - \frac{\nu_{12}^2}{E_1} \right)$ , which can be shown to be equivalent to  $\Lambda_{22}^0 = 2 \frac{1 - \nu_{12}\nu_{21}}{E_2}$  by recalling that  $\nu_{21} = \frac{E_2}{E_1} \nu_{12}$ .

between the Stress Intensity Factor (SIF)  $K$  and Energy Release Rate (ERR)  
 100  $G$  of a generic configuration of structural and crack geometry and the solution  
 for a Center Crack (CC) in an infinite plate

$$K_{CC} = \sigma\sqrt{a} \quad \text{or} \quad G_{CC} = \frac{\sigma^2}{E}a, \quad (14)$$

where the crack size is  $2a$ . It thus seems reasonable to look for a functional  
 form of  $f(\Delta\theta)$  in Eq. 11 and Eq. 12 among known analytical solutions of SIFs  
 and ERRs and such that a physically-meaningful similarity between the two  
 105 configurations could be established.

- **Straight central crack in an infinite isotropic plate under far-field transverse tension [25].**

$$f_I(\Delta\theta) = \sin(\Delta\theta) \quad f_{II}(\Delta\theta) = 0 \quad (15)$$

It is the simplest choice, based on considering the debond chord  $2R_f \sin \Delta\theta$   
 as its representative size. However, as apparent in Eq. 15, there is no  
 110 Mode II geometry correction factor available (a straight crack in transverse  
 tension propagates only in Mode I) and it is thus not suited to establish a  
 relation of similarity with debond ERR, which is Mode II dominated for  
 large  $\Delta\theta$ .

- **Inclined central crack in an infinite isotropic plate under far-field tension [25].**

115

$$\begin{aligned} f_I(\Delta\theta) &= \sin(\Delta\theta) \sin^4\left(\frac{\pi}{2} - \Delta\theta\right) \\ f_{II}(\Delta\theta) &= \sin(\Delta\theta) \sin^2\left(\frac{\pi}{2} - \Delta\theta\right) \cos^2\left(\frac{\pi}{2} - \Delta\theta\right) \end{aligned} \quad (16)$$

A first attempt to amend the shortcomings of Eq. 15 is to consider the  
 geometry correction factor of the inclined crack subjected to transverse  
 load. However,  $f_{II}(90^\circ) = 0$  in Eq. 16, which makes also this choice not  
 a good choice to establish a similarity relation with debond ERR (Mode  
 120 II ERR is well-defined and different from 0 at  $\Delta\theta = 90^\circ$  for debonds).

- **Circular crack in an infinite isotropic plate under far-field tension transverse to crack's chord [27].**

$$\begin{aligned}
f_I(\Delta\theta) &= \frac{G_I}{\sigma_{ref}\varepsilon_{ref}R} = \frac{1}{2} \sin(\Delta\theta) \times \\
&\times \left( \frac{1 - \sin^2\left(\frac{\Delta\theta}{2}\right) \cos^2\left(\frac{\Delta\theta}{2}\right)}{1 + \sin^2\left(\frac{\Delta\theta}{2}\right)} \cos\left(\frac{\Delta\theta}{2}\right) + \cos\left(\frac{3}{2}\Delta\theta\right) \right)^2 \\
f_{II}(\Delta\theta) &= \frac{G_{II}}{\sigma_{ref}\varepsilon_{ref}R} = \frac{1}{2} \sin(\Delta\theta) \times \\
&\times \left( \frac{1 - \sin^2\left(\frac{\Delta\theta}{2}\right) \cos^2\left(\frac{\Delta\theta}{2}\right)}{1 + \sin^2\left(\frac{\Delta\theta}{2}\right)} \sin\left(\frac{\Delta\theta}{2}\right) + \sin\left(\frac{3}{2}\Delta\theta\right) \right)^2
\end{aligned} \tag{17}$$

125 The geometry correction factors of Eq. 17 (shown in Fig. 1) present a solution to the issues characterising Eq. 15 and Eq. 16: Mode II is defined and both modes are defined and continuous for  $\Delta\theta = 0^\circ - 180^\circ$ . By evaluating the elastic properties  $E_2$ ,  $\nu_{12}$  and  $\nu_{21}$  at the value of  $V_f$  of the composite under consideration and substituting Eq. 17 in Eq. 12 and Eq. 11, we obtain the Mode I  $G_{I0}$  and Mode II  $G_{II0}$  ERR of a circular crack of size  $a = 2\Delta\theta$  in an infinite isotropic medium, which has properties

130 equivalent to the elastic properties of a UD composite of fiber volume fraction  $V_f$  in its plane of transverse isotropy, obtained by application of the Concentric Cylinders Assembly [28] with Self-Consistent Shear [29] (CCA-SCS) model. The following expressions are derived,

1. under plane strain conditions and applied far-field transverse strain:

$$\begin{aligned}
G_{I0} &= f_I(\Delta\theta) \frac{E_2(V_f)}{1 - \nu_{12}(V_f)\nu_{21}(V_f)} \varepsilon_0^2 R_f \\
G_{II0} &= f_{II}(\Delta\theta) \frac{E_2}{1 - \nu_{12}\nu_{21}} \varepsilon_0^2 R_f;
\end{aligned} \tag{18}$$

- 135 2. under plane strain conditions and applied far-field transverse stress:

$$\begin{aligned}
G_{I0} &= f_I(\Delta\theta) \frac{1 - \nu_{12}(V_f)\nu_{21}(V_f)}{E_2(V_f)} \sigma_0^2 R_f \\
G_{II0} &= f_{II}(\Delta\theta) \frac{1 - \nu_{12}(V_f)\nu_{21}(V_f)}{E_2(V_f)} \sigma_0^2 R_f
\end{aligned} \tag{19}$$

3. under plane stress conditions and applied far-field transverse strain:

$$\begin{aligned} G_{I0} &= f_I(\Delta\theta) E_2(V_f) \varepsilon_0^2 R_f \\ G_{II0} &= f_{II}(\Delta\theta) E_2(V_f) \varepsilon_0^2 R_f \end{aligned} \quad (20)$$

4. under plane stress conditions and applied far-field transverse stress:

$$\begin{aligned} G_{I0} &= f_I(\Delta\theta) \frac{\sigma_0^2}{E_2(V_f)} R_f \\ G_{II0} &= f_{II}(\Delta\theta) \frac{\sigma_0^2}{E_2(V_f)} R_f \end{aligned} \quad (21)$$

This configuration thus establishes a physically-meaningful relation of similarity, as the ratios  $\frac{G_I}{G_{I0}} = g_I(\Delta\theta, V_f) [-]$  and  $\frac{G_{II}}{G_{II0}} = g_{II}(\Delta\theta, V_f) [-]$  measure the effect of: the mismatch in elastic properties between phases (in Eq. 17 the medium is isotropic); the finite size of the geometry (in Eq. 17 the medium is infinite); the interaction with neighboring undamaged and partially debonded fibers, a free surface (in UD composites) or the  $0^\circ/90^\circ$  interface (in cross-ply laminates).

Given that debond ERR for RVEs presented in Section ?? is evaluated under conditions of plane strain and applied transverse strain, the expressions of  $G_{I0}$  and  $G_{II0}$  in Eq. 18 are adopted in the following.

## 5. Effect of elastic properties mismatch

## 6. Effect of fiber volume fraction

## 7. Effect of neighboring fibers

## References

- [1] A. Kopp, S. Stappert, D. Mattsson, K. Olofsson, E. Marklund, G. Kurth, E. Mooij, E. Roorda, The aurora space launcher concept, CEAS Space Journal 10 (2) (2017) 167–187. doi:10.1007/s12567-017-0184-2.



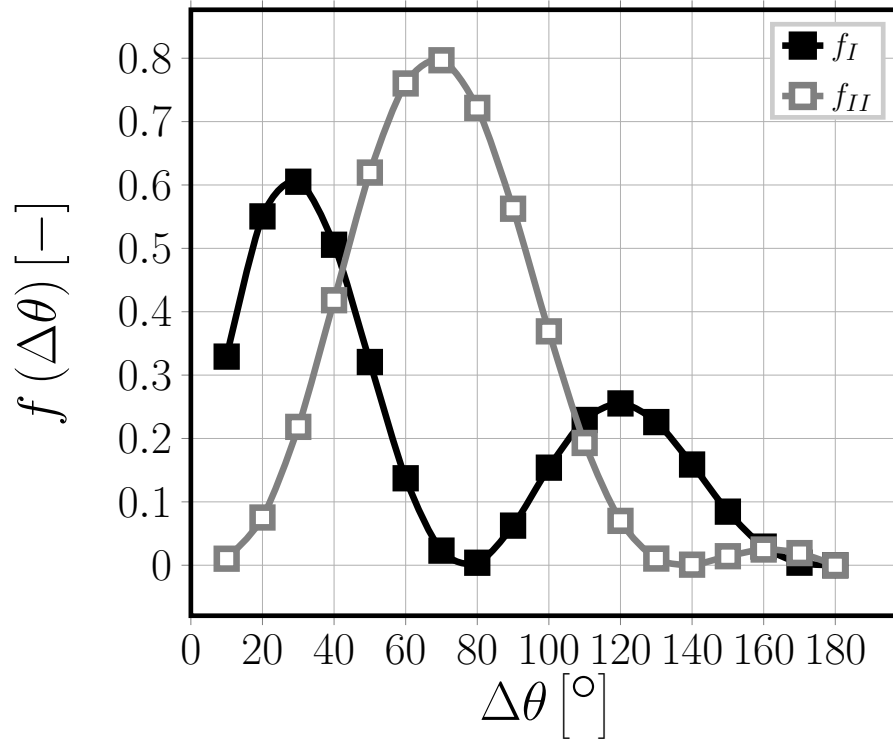


Figure 1: Mode I ( $f_I$ ) and Mode II ( $f_{II}$ ) geometry correction functions for a circular crack in infinite isotropic medium. The chord of the crack is normal to the loading direction and the crack size is  $a = 2\Delta\theta$ .

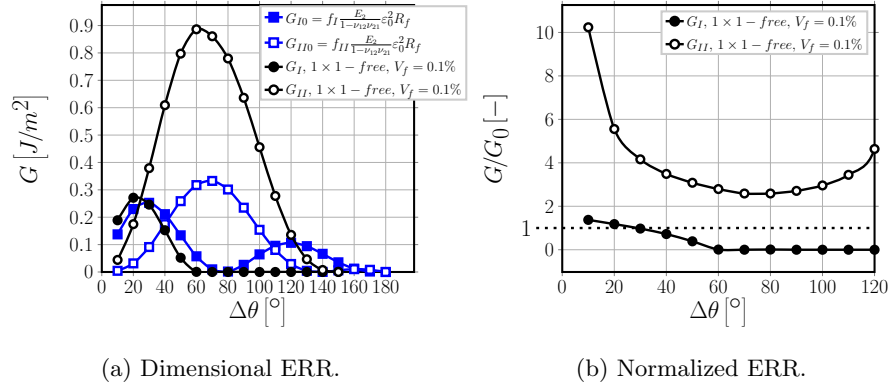


Figure 2: *Left*: Mode I and Mode II ERR for the circular crack in an infinite isotropic medium ( $G_{I0}$  and  $G_{II0}$ ) and for a single partially debonded fiber in an infinite matrix ( $1 \times 1 - free$ ,  $V_f = 0.1\%$ ). In  $G_{I0}$  and  $G_{II0}$ ,  $E_2$ ,  $\nu_{12}$  and  $\nu_{21}$  are evaluated using the Concentric Cylinders Assembly [28] with Self-Consistent Shear [29] (CCA-SCS) model for  $V_f = 0.1\%$ . In both cases, a transverse load is applied in the form of transverse strain  $\varepsilon_x$  of 1%. *Right*: Mode I and Mode II ERR of single partially debonded fiber in an infinite matrix ( $1 \times 1 - free$ ,  $V_f = 0.1\%$ ) normalized by Mode I and Mode II ERR of the circular crack in an infinite isotropic medium ( $G_{I0}$  and  $G_{II0}$ ).

- [2] J. Cugnoni, R. Amacher, S. Kohler, J. Brunner, E. Kramer, C. Dransfeld, W. Smith, K. Scobbie, L. Sorensen, J. Botsis, Towards aerospace grade thin-ply composites: Effect of ply thickness, fibre, matrix and interlayer toughening on strength and damage tolerance, *Composites Science and Technology* 168 (2018) 467–477. doi:10.1016/j.compscitech.2018.08.037.
- [3] H. Sasayama, K. Kawabe, S. Tomoda, I. Ohsawa, K. Kageyama, N. Ogata, Effect of lamina thickness on first ply failure in multidirectionally laminated composites, in: *Proceedings of the 8<sup>th</sup> Japan SAMPE Symposium*, SAMPE, 2003.
- [4] H. Saito, H. Takeuchi, I. Kimpara, Experimental evaluation of the damage growth restraining in 90 layer of thin-ply cfrp cross-ply laminates, *Advanced Composite Materials* 21 (1) (2012) 57–66. doi:10.1163/156855112X629522.

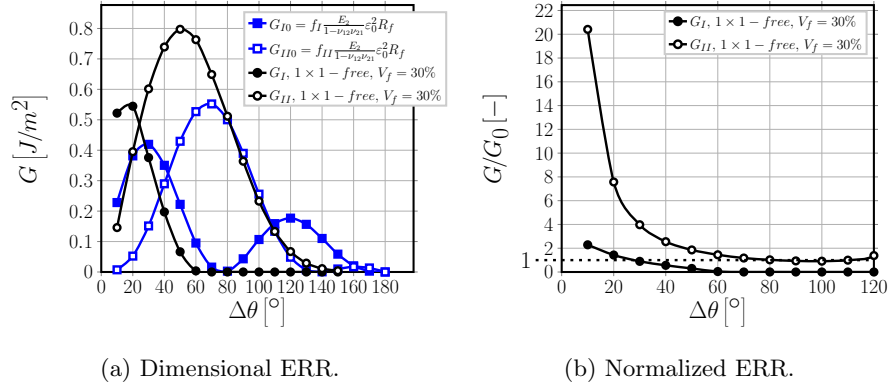


Figure 3: *Left*: Mode I and Mode II ERR for the circular crack in an infinite isotropic medium ( $G_{I0}$  and  $G_{II0}$ ) and for a single partially debonded fiber in an infinite matrix ( $1 \times 1 - free$ ,  $V_f = 30\%$ ). In  $G_{I0}$  and  $G_{II0}$ ,  $E_2$ ,  $\nu_{12}$  and  $\nu_{21}$  are evaluated using the Concentric Cylinders Assembly [28] with Self-Consistent Shear [29] (CCA-SCS) model for  $V_f = 30\%$ . In both cases, a transverse load is applied in the form of transverse strain  $\varepsilon_x$  of 1%. *Right*: Mode I and Mode II ERR of single partially debonded fiber in an infinite matrix ( $1 \times 1 - free$ ,  $V_f = 30\%$ ) normalized by Mode I and Mode II ERR of the circular crack in an infinite isotropic medium ( $G_{I0}$  and  $G_{II0}$ ).

- [5] R. Amacher, J. Cugnoni, J. Botsis, L. Sorensen, W. Smith, C. Dransfeld, Thin ply composites: Experimental characterization and modeling of size-effects, Composites Science and Technology 101 (2014) 121–132. doi:10.1016/j.compscitech.2014.06.027.
- [6] J. E. Bailey, P. T. Curtis, A. Parvizi, On the transverse cracking and longitudinal splitting behaviour of glass and carbon fibre reinforced epoxy cross ply laminates and the effect of poisson and thermally generated strain, Proceedings of the Royal Society A: Mathematical, Physical and Engineering Sciences 366 (1727) (1979) 599–623. doi:10.1098/rspa.1979.0071.
- [7] J. E. Bailey, A. Parvizi, On fibre debonding effects and the mechanism of transverse-ply failure in cross-ply laminates of glass fibre/thermoset composites, Journal of Materials Science 16 (3) (1981) 649–659. doi:10.1007/bf02402782.

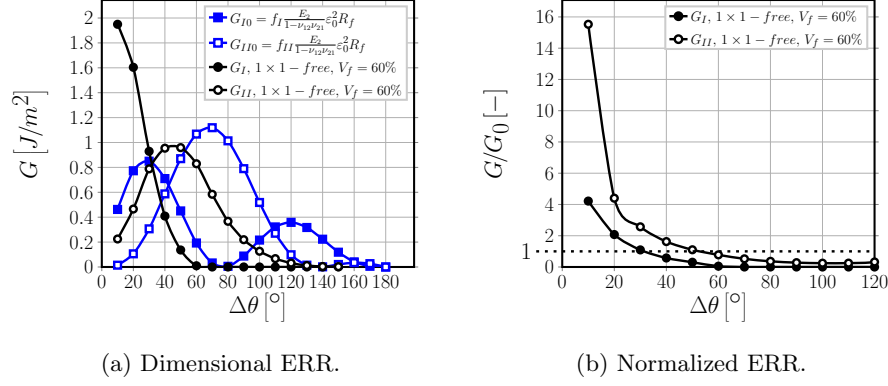


Figure 4: *Left*: Mode I and Mode II ERR for the circular crack in an infinite isotropic medium ( $G_{I0}$  and  $G_{II0}$ ) and for a single partially debonded fiber in an infinite matrix ( $1 \times 1 - free$ ,  $V_f = 60\%$ ). In  $G_{I0}$  and  $G_{II0}$ ,  $E_2$ ,  $\nu_{12}$  and  $\nu_{21}$  are evaluated using the Concentric Cylinders Assembly [28] with Self-Consistent Shear [29] (CCA-SCS) model for  $V_f = 60\%$ . In both cases, a transverse load is applied in the form of transverse strain  $\varepsilon_x$  of 1%. *Right*: Mode I and Mode II ERR of single partially debonded fiber in an infinite matrix ( $1 \times 1 - free$ ,  $V_f = 60\%$ ) normalized by Mode I and Mode II ERR of the circular crack in an infinite isotropic medium ( $G_{I0}$  and  $G_{II0}$ ).

[8] L. Asp, L. Berglund, R. Talreja, Prediction of matrix-initiated transverse failure in polymer composites, Composites Science and Technology 56 (9) (1996) 1089–1097. doi:10.1016/0266-3538(96)00074-7.

185 [9] J. A. Kies, Maximum strains in the resin of fibreglass composites, Nrl report 5752, ad-274560, Washington (DC): U.S. Naval Research Laboratory (1962).

[10] H. Zhang, M. Ericson, J. Varna, L. Berglund, Transverse single-fibre test for interfacial debonding in composites: 1. experimental observations, Composites Part A: Applied Science and Manufacturing 28 (4) (1997) 309–315. doi:10.1016/s1359-835x(96)00123-6.

190 [11] F. París, E. Correa, V. Mantić, Kinking of transversal interface cracks between fiber and matrix, Journal of Applied Mechanics 74 (4) (2007) 703. doi:10.1115/1.2711220.

- 195 [12] L. Zhuang, R. Talreja, J. Varna, Transverse crack formation in unidirectional composites by linking of fibre/matrix debond cracks, *Composites Part A: Applied Science and Manufacturing* 107 (2018) 294–303. doi:10.1016/j.compositesa.2018.01.013.
- [13] L. Zhuang, A. Pupurs, J. Varna, R. Talreja, Z. Ayadi, Effects of inter-fiber  
200 spacing on fiber-matrix debond crack growth in unidirectional composites under transverse loading, *Composites Part A: Applied Science and Manufacturing* 109 (2018) 463–471. doi:10.1016/j.compositesa.2018.03.031.
- [14] C. Sandino, E. Correa, F. París, Numerical analysis of the influence of a  
205 nearby fibre on the interface crack growth in composites under transverse tensile load, *Engineering Fracture Mechanics* 168 (2016) 58–75. doi:10.1016/j.engfracmech.2016.01.022.
- [15] J. Varna, L. Q. Zhuang, A. Pupurs, Z. Ayadi, Growth and interaction of debonds in local clusters of fibers in unidirectional composites during  
210 transverse loading, *Key Engineering Materials* 754 (2017) 63–66. doi:10.4028/www.scientific.net/kem.754.63.
- [16] C. Sandino, E. Correa, F. París, Interface crack growth under transverse compression: nearby fibre effect, in: *Proceeding of the 18<sup>th</sup> European Conference on Composite Materials (ECCM-18)*, 2018.
- 215 [17] M. Comninou, The interface crack, *Journal of Applied Mechanics* 44 (4) (1977) 631. doi:10.1115/1.3424148.
- [18] M. Toya, A crack along the interface of a circular inclusion embedded in an infinite solid, *Journal of the Mechanics and Physics of Solids* 22 (5) (1974) 325–348. doi:10.1016/0022-5096(74)90002-7.
- 220 [19] F. París, J. C. Caño, J. Varna, The fiber-matrix interface crack — a numerical analysis using boundary elements, *International Journal of Fracture* 82 (1) (1996) 11–29. doi:10.1007/bf00017861.

- [20] S. P. Timoshenko, J. N. Goodier, Theory of elasticity, Engineering societies monographs, McGraw-Hill, 1987.
- 225 [21] V. Mantič, Interface crack onset at a circular cylindrical inclusion under a remote transverse tension. application of a coupled stress and energy criterion, International Journal of Solids and Structures 46 (6) (2009) 1287–1304. doi:10.1016/j.ijsolstr.2008.10.036.
- 230 [22] P. P. Camanho, C. G. Dvila, S. T. Pinho, L. Iannucci, P. Robinson, Prediction of in situ strengths and matrix cracking in composites under transverse tension and in-plane shear, Composites Part A: Applied Science and Manufacturing 37 (2) (2006) 165 – 176, compTest 2004. doi:10.1016/j.compositesa.2005.04.023.
- 235 [23] N. Laws, G. Dvorak, M. Hejazi, Stiffness changes in unidirectional composites caused by crack systems, Mechanics of Materials 2 (2) (1983) 123 – 137. doi:10.1016/0167-6636(83)90032-7.
- 240 [24] J. Varna, 2.10 crack separation based models for microcracking, in: P. W. Beaumont, C. H. Zweben (Eds.), Comprehensive Composite Materials II, Elsevier, Oxford, 2018, pp. 192 – 220. doi:10.1016/B978-0-12-803581-8.09910-0.
- [25] H. Tada, P. Paris, G. Irwin, The Stress Analysis of Cracks Handbook, ASME Press, 2000.
- 245 [26] G. I. Barenblatt, Scaling phenomena in fatigue and fracture, International Journal of Fracture 138 (1-4) (2006) 19–35. doi:10.1007/s10704-006-0036-0.
- [27] N. I. Ioakmidis, P. S. Theocaris, Array of periodic curvilinear cracks in an infinite isotropic medium, Acta Mechanica 28 (1) (1977) 239–254. doi:10.1007/BF01208801.
- 250 [28] Z. Hashin, Analysis of composite materials—a survey, Journal of Applied Mechanics 50 (3) (1983) 481. doi:10.1115/1.3167081.

- [29] R. Christensen, K. Lo, Solutions for effective shear properties in three phase sphere and cylinder models, *Journal of the Mechanics and Physics of Solids* 27 (4) (1979) 315–330. doi:10.1016/0022-5096(79)90032-2.

## **8. Conclusions**